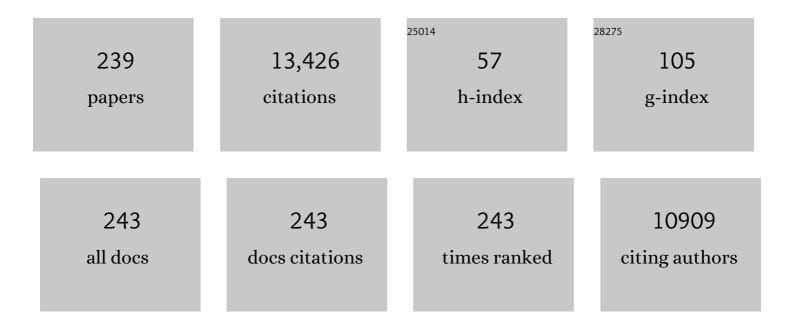
List of Publications by Year in descending order

Source: https://exaly.com/author-pdf/5908864/publications.pdf Version: 2024-02-01



ANKED D IENCEN

#	Article	IF	CITATIONS
1	A review of catalytic upgrading of bio-oil to engine fuels. Applied Catalysis A: General, 2011, 407, 1-19.	2.2	1,414
2	Oxy-fuel combustion of solid fuels. Progress in Energy and Combustion Science, 2010, 36, 581-625.	15.8	940
3	Fuel nitrogen conversion in solid fuel fired systems. Progress in Energy and Combustion Science, 2003, 29, 89-113.	15.8	764
4	Catalytic steam reforming of bio-oil. International Journal of Hydrogen Energy, 2012, 37, 6447-6472.	3.8	349
5	Screening of Catalysts for Hydrodeoxygenation of Phenol as a Model Compound for Bio-oil. ACS Catalysis, 2013, 3, 1774-1785.	5.5	348
6	TG-FTIR Study of the Influence of Potassium Chloride on Wheat Straw Pyrolysis. Energy & Fuels, 1998, 12, 929-938.	2.5	261
7	Mn/TiO2 and Mn–Fe/TiO2 catalysts synthesized by deposition precipitation—promising for selective catalytic reduction of NO with NH3 at low temperatures. Applied Catalysis B: Environmental, 2015, 165, 628-635.	10.8	241
8	CO hydrogenation to methanol on Cu–Ni catalysts: Theory and experiment. Journal of Catalysis, 2012, 293, 51-60.	3.1	195
9	Transportation fuels from biomass fast pyrolysis, catalytic hydrodeoxygenation, and catalytic fast hydropyrolysis. Progress in Energy and Combustion Science, 2018, 68, 268-309.	15.8	194
10	Deactivation of V2O5-WO3-TiO2 SCR catalyst at a biomass-fired combined heat and power plant. Applied Catalysis B: Environmental, 2005, 60, 253-264.	10.8	186
11	Review of technologies for mercury removal from flue gas from cement production processes. Progress in Energy and Combustion Science, 2012, 38, 599-629.	15.8	183
12	Numerical modeling of straw combustion in a fixed bed. Fuel, 2005, 84, 389-403.	3.4	181
13	Two-fluid spray atomisation and pneumatic nozzles for fluid bed coating/agglomeration purposes: A review. Chemical Engineering Science, 2008, 63, 3821-3842.	1.9	176
14	Formation of polycyclic aromatic hydrocarbons and soot in fuel-rich oxidation of methane in a laminar flow reactor. Combustion and Flame, 2004, 136, 91-128.	2.8	157
15	Ash transformation during co-firing coal and straw. Fuel, 2007, 86, 1008-1020.	3.4	153
16	Modelling and experiments of straw combustion in a grate furnace. Biomass and Bioenergy, 2000, 19, 199-208.	2.9	143
17	High-temperature entrained flow gasification of biomass. Fuel, 2012, 93, 589-600.	3.4	132
18	Deactivation of V2O5-WO3-TiO2 SCR catalyst at biomass fired power plants: Elucidation of mechanisms by lab- and pilot-scale experiments. Applied Catalysis B: Environmental, 2008, 83, 186-194.	10.8	131

#	Article	IF	CITATIONS
19	Promoted V 2 O 5 /TiO 2 catalysts for selective catalytic reduction of NO with NH 3 at low temperatures. Applied Catalysis B: Environmental, 2016, 183, 282-290.	10.8	129
20	Influence on nickel particle size on the hydrodeoxygenation of phenol over Ni/SiO 2. Catalysis Today, 2016, 259, 277-284.	2.2	126
21	Laboratory Investigation of Selective Catalytic Reduction Catalysts:Â Deactivation by Potassium Compounds and Catalyst Regeneration. Industrial & Engineering Chemistry Research, 2004, 43, 941-947.	1.8	120
22	Direct upgrading of fast pyrolysis lignin vapor over the HZSM-5 catalyst. Green Chemistry, 2016, 18, 1965-1975.	4.6	117
23	Effects of H2S and process conditions in the synthesis of mixed alcohols from syngas over alkali promoted cobalt-molybdenum sulfide. Applied Catalysis A: General, 2009, 366, 29-43.	2.2	108
24	Experimental methods and modeling techniques for description of cell population heterogeneity. Biotechnology Advances, 2011, 29, 575-599.	6.0	108
25	A review of the interference of carbon containing fly ash with air entrainment in concrete. Progress in Energy and Combustion Science, 2008, 34, 135-154.	15.8	106
26	Activity and stability of Mo2C/ZrO2 as catalyst for hydrodeoxygenation of mixtures of phenol and 1-octanol. Journal of Catalysis, 2015, 328, 208-215.	3.1	100
27	Ketene as a Reaction Intermediate in the Carbonylation of Dimethyl Ether to Methyl Acetate over Mordenite. Angewandte Chemie - International Edition, 2015, 54, 7261-7264.	7.2	98
28	The Influence of Inorganic Materials on the Thermal Deactivation of Fuel Chars. Energy & Fuels, 2001, 15, 1110-1122.	2.5	97
29	Reversible and irreversible deactivation of Cu-CHA NH3-SCRcatalysts by SO2 and SO3. Applied Catalysis B: Environmental, 2018, 226, 38-45.	10.8	97
30	Ammonia conversion and NOx formation in laminar coflowing nonpremixed methane-air flames. Combustion and Flame, 2002, 131, 285-298.	2.8	95
31	Influence of fast pyrolysis conditions on yield and structural transformation of biomass chars. Fuel Processing Technology, 2015, 140, 205-214.	3.7	94
32	Solvent optimization for efficient enzymatic monoacylglycerol production based on a glycerolysis reaction. JAOCS, Journal of the American Oil Chemists' Society, 2005, 82, 559-564.	0.8	93
33	Biomass Gasification Behavior in an Entrained Flow Reactor: Gas Product Distribution and Soot Formation. Energy & Fuels, 2012, 26, 5992-6002.	2.5	93
34	An experimental study of biomass ignitionâ <sup>~</sup> †. Fuel, 2003, 82, 825-833.	3.4	92
35	Formation and reduction of nitric oxide in fixed-bed combustion of straw. Fuel, 2006, 85, 705-716.	3.4	90
36	Coal devolatilization and char conversion under suspension fired conditions in O2/N2 and O2/CO2 atmospheres. Fuel, 2010, 89, 3373-3380.	3.4	86

#	Article	IF	CITATIONS
37	Effects of several types of biomass fuels on the yield, nanostructure and reactivity of soot from fast pyrolysis at high temperatures. Applied Energy, 2016, 171, 468-482.	5.1	82
38	Deactivation of vanadia-based commercial SCR catalysts by polyphosphoric acids. Applied Catalysis B: Environmental, 2008, 83, 110-122.	10.8	79
39	Experimental study of char thermal deactivation. Fuel, 2002, 81, 1065-1075.	3.4	76
40	Formation and reduction of NOx in pressurized fluidized bed combustion of coal. Fuel, 1995, 74, 1555-1569.	3.4	74
41	Steam reforming of cyclic model compounds of bio-oil over Ni-based catalysts: Product distribution and carbon formation. Applied Catalysis B: Environmental, 2015, 165, 117-127.	10.8	70
42	Stability and resistance of nickel catalysts for hydrodeoxygenation: carbon deposition and effects of sulfur, potassium, and chlorine in the feed. Catalysis Science and Technology, 2014, 4, 3672-3686.	2.1	69
43	A kinetic study of gaseous potassium capture by coal minerals in a high temperature fixed-bed reactor. Fuel, 2008, 87, 3304-3312.	3.4	64
44	Heteropoly acid promoted V2O5/TiO2 catalysts for NO abatement with ammonia in alkali containing flue gases. Catalysis Science and Technology, 2011, 1, 631.	2.1	64
45	Characterization of free radicals by electron spin resonance spectroscopy in biochars from pyrolysis at high heating rates and at high temperatures. Biomass and Bioenergy, 2016, 94, 117-129.	2.9	64
46	Evaluation of different oxygen carriers for biomass tar reforming (I): Carbon deposition in experiments with toluene. Fuel, 2011, 90, 1049-1060.	3.4	63
47	Suspension Combustion of Wood: Influence of Pyrolysis Conditions on Char Yield, Morphology, and Reactivity. Energy & Fuels, 2008, 22, 2955-2962.	2.5	62
48	Deactivation of Ni-MoS2 by bio-oil impurities during hydrodeoxygenation of phenol and octanol. Applied Catalysis A: General, 2016, 523, 159-170.	2.2	62
49	Effect of fast pyrolysis conditions on biomass solid residues at high temperatures. Fuel Processing Technology, 2016, 143, 118-129.	3.7	62
50	Evaluation of Binary Solvent Mixtures for Efficient Monoacylglycerol Production by Continuous Enzymatic Glycerolysis. Journal of Agricultural and Food Chemistry, 2006, 54, 7113-7119.	2.4	61
51	Evaluation of different oxygen carriers for biomass tar reforming (II): Carbon deposition in experiments with methane and other gases. Fuel, 2011, 90, 1370-1382.	3.4	61
52	Hydrodeoxygenation of Phenol to Benzene and Cyclohexane on Rh(111) and Rh(211) Surfaces: Insights from Density Functional Theory. Journal of Physical Chemistry C, 2016, 120, 18529-18537.	1.5	61
53	Importance of the Cu oxidation state for the SO2-poisoning of a Cu-SAPO-34 catalyst in the NH3-SCR reaction. Applied Catalysis B: Environmental, 2018, 236, 377-383.	10.8	61
54	Inâ€Situ Observation of Cu–Ni Alloy Nanoparticle Formation by Xâ€Ray Diffraction, Xâ€Ray Absorption Spectroscopy, and Transmission Electron Microscopy: Influence of Cu/Ni Ratio. ChemCatChem, 2014, 6, 301-310.	1.8	60

#	Article	IF	CITATIONS
55	Visualizing the mobility of silver during catalytic soot oxidation. Applied Catalysis B: Environmental, 2016, 183, 28-36.	10.8	60
56	Steam reforming of ethanol: Effects of support and additives on Ni-based catalysts. International Journal of Hydrogen Energy, 2013, 38, 15105-15118.	3.8	59
57	Reduction of NO over Wheat Straw Char. Energy & Fuels, 2001, 15, 1359-1368.	2.5	58
58	Comparison of high temperature chars of wheat straw and rice husk with respect to chemistry, morphology and reactivity. Biomass and Bioenergy, 2016, 86, 76-87.	2.9	57
59	Retention of Organic Elements during Solid Fuel Pyrolysis with Emphasis on the Peculiar Behavior of Nitrogen. Energy & Fuels, 2005, 19, 1631-1643.	2.5	56
60	Model based analysis of the drying of a single solution droplet in an ultrasonic levitator. Chemical Engineering Science, 2006, 61, 2701-2709.	1.9	56
61	Reaction mechanism of dimethyl ether carbonylation to methyl acetate over mordenite – a combined DFT/experimental study. Catalysis Science and Technology, 2017, 7, 1141-1152.	2.1	54
62	Impact of SO2-poisoning over the lifetime of a Cu-CHA catalyst for NH3-SCR. Applied Catalysis B: Environmental, 2018, 238, 104-110.	10.8	54
63	Kinetic Study of NO Reduction over Biomass Char under Dynamic Conditions. Energy & Fuels, 2003, 17, 1429-1436.	2.5	52
64	Plasma-catalytic dry reforming of methane: Screening of catalytic materials in a coaxial packed-bed DBD reactor. Chemical Engineering Journal, 2020, 397, 125519.	6.6	52
65	A Comparison of Coal Char Reactivity Determined from Thermogravimetric and Laminar Flow Reactor Experiments. Energy & Fuels, 1998, 12, 268-276.	2.5	50
66	Influence of reaction products of K-getter fuel additives on commercial vanadia-based SCR catalysts. Applied Catalysis B: Environmental, 2009, 86, 196-205.	10.8	50
67	Production of heat-sensitive monoacylglycerols by enzymatic glycerolysis in tert -pentanol: Process optimization by response surface methodology. JAOCS, Journal of the American Oil Chemists' Society, 2006, 83, 27-33.	0.8	48
68	Catalytic Conversion of Syngas into Higher Alcohols over Carbide Catalysts. Industrial & Engineering Chemistry Research, 2012, 51, 4161-4172.	1.8	48
69	Effects of Feed Composition and Feed Impurities in the Catalytic Conversion of Syngas to Higher Alcohols over Alkali-Promoted Cobalt–Molybdenum Sulfide. Industrial & Engineering Chemistry Research, 2011, 50, 7949-7963.	1.8	44
70	Atmospheric Hydrodeoxygenation of Biomass Fast Pyrolysis Vapor by MoO <sub>3</sub> . ACS Sustainable Chemistry and Engineering, 2016, 4, 5432-5440.	3.2	44
71	Supported molybdenum carbide for higher alcohol synthesis from syngas. Catalysis Today, 2013, 215, 162-168.	2.2	43
72	Probing the Active Sites of MoS <sub>2</sub> Based Hydrotreating Catalysts Using Modulation Excitation Spectroscopy. ACS Catalysis, 2019, 9, 2568-2579.	5.5	43

#	Article	IF	CITATIONS
73	A Model for Nitrogen Chemistry in Oxy-Fuel Combustion of Pulverized Coal. Energy & Fuels, 2011, 25, 4280-4289.	2.5	42
74	Selective oxidation of propylene to acrolein by hydrothermally synthesized bismuth molybdates. Applied Catalysis A: General, 2014, 482, 145-156.	2.2	41
75	NH3 oxidation catalysed by calcined limestone—a kinetic study. Fuel, 2002, 81, 1871-1881.	3.4	40
76	Experimental and Modeling Study of Biomass Reburning. Energy & amp; Fuels, 2004, 18, 1442-1450.	2.5	39
77	Thermal Dissociation of SO3at 1000â^'1400 Kâ€. Journal of Physical Chemistry A, 2006, 110, 6654-6659.	1.1	39
78	Influence of reaction products of K-getter fuel additives on commercial vanadia-based SCR catalysts. Applied Catalysis B: Environmental, 2009, 86, 206-215.	10.8	39
79	Flame spray synthesis of CoMo/Al2O3 hydrotreating catalysts. Applied Catalysis A: General, 2011, 397, 201-208.	2.2	39
80	Characterization of Residual Particulates from Biomass Entrained Flow Gasification. Energy & Fuels, 2013, 27, 262-270.	2.5	39
81	Optimization of a new flow design for solid oxide cells using computational fluid dynamics modelling. Journal of Power Sources, 2016, 336, 261-271.	4.0	39
82	Bismuth Molybdate Catalysts Prepared by Mild Hydrothermal Synthesis: Influence of pH on the Selective Oxidation of Propylene. Catalysts, 2015, 5, 1554-1573.	1.6	38
83	Effect of NO2 and water on the catalytic oxidation of soot. Applied Catalysis B: Environmental, 2017, 205, 182-188.	10.8	38
84	Impact of ZSM-5 Deactivation on Bio-Oil Quality during Upgrading of Straw Derived Pyrolysis Vapors. Energy & Fuels, 2019, 33, 397-412.	2.5	38
85	A perspective on catalytic hydropyrolysis of biomass. Renewable and Sustainable Energy Reviews, 2021, 143, 110960.	8.2	38
86	Bifunctional Synergy in CO Hydrogenation to Methanol with Supported Cu. Catalysis Letters, 2020, 150, 1427-1433.	1.4	37
87	One-step synthesis of bismuth molybdate catalysts via flame spray pyrolysis for the selective oxidation of propylene to acrolein. Chemical Communications, 2014, 50, 15404-15406.	2.2	36
88	Importance of the oxygen bond strength for catalytic activity in soot oxidation. Applied Catalysis B: Environmental, 2016, 188, 235-244.	10.8	36
89	The Effect of Pt Particle Size on the Oxidation of CO, C3H6, and NO Over Pt/Al2O3 for Diesel Exhaust Aftertreatment. Topics in Catalysis, 2017, 60, 1333-1344.	1.3	36
90	The roles of CO and CO2 in high pressure methanol synthesis over Cu-based catalysts. Journal of Catalysis, 2021, 393, 324-334.	3.1	36

#	Article	IF	CITATIONS
91	Hydrogen assisted catalytic biomass pyrolysis. Effect of temperature and pressure. Biomass and Bioenergy, 2018, 115, 97-107.	2.9	35
92	Enhancing bio-oil quality and energy recovery by atmospheric hydrodeoxygenation of wheat straw pyrolysis vapors using Pt and Mo-based catalysts. Sustainable Energy and Fuels, 2020, 4, 1991-2008.	2.5	35
93	A study of benzene formation in a laminar flow reactor. Proceedings of the Combustion Institute, 2002, 29, 1329-1336.	2.4	33
94	Performance of diesel particulate filter catalysts in the presence of biodiesel ash species. Fuel, 2013, 106, 234-240.	3.4	33
95	Hydrodeoxygenation of phenol over Pd catalysts by in-situ generated hydrogen from aqueous reforming of formic acid. Catalysis Communications, 2016, 82, 46-49.	1.6	33
96	Sulfation of Condensed Potassium Chloride by SO <sub>2</sub> . Energy & Fuels, 2013, 27, 3283-3289.	2.5	32
97	Influence of preparation method on supported Cu–Ni alloys and their catalytic properties in high pressure CO hydrogenation. Catalysis Science and Technology, 2014, 4, 378-386.	2.1	32
98	NO Formation during Oxy-Fuel Combustion of Coal and Biomass Chars. Energy & Fuels, 2014, 28, 4684-4693.	2.5	32
99	Deactivation behavior of an iron-molybdate catalyst during selective oxidation of methanol to formaldehyde. Catalysis Science and Technology, 2018, 8, 4626-4637.	2.1	32
100	Steam reforming of light oxygenates. Catalysis Science and Technology, 2013, 3, 3292.	2.1	31
101	Influence of H 2 O and H 2 S on the composition, activity, and stability of sulfided Mo, CoMo, and NiMo supported on MgAl 2 O 4 for hydrodeoxygenation of ethylene glycol. Applied Catalysis A: General, 2018, 551, 106-121.	2.2	31
102	Deoxygenation of wheat straw fast pyrolysis vapors over Na-Al2O3 catalyst for production of bio-oil with low acidity. Chemical Engineering Journal, 2020, 394, 124878.	6.6	31
103	Propargyl recombination: estimation of the high temperature, low pressure rate constant from flame measurements. Proceedings of the Combustion Institute, 2005, 30, 1023-1031.	2.4	30
104	The effect of combustion conditions in a full-scale low-NOx coal fired unit on fly ash properties for its application in concrete mixtures. Fuel Processing Technology, 2009, 90, 180-185.	3.7	30
105	Structure of alumina supported vanadia catalysts for oxidative dehydrogenation of propane prepared by flame spray pyrolysis. Applied Catalysis A: General, 2013, 451, 207-215.	2.2	30
106	Continuous Catalytic Hydrodeoxygenation of Guaiacol over Pt/SiO2 and Pt/H-MFI-90. Catalysts, 2015, 5, 1152-1166.	1.6	30
107	Catalytic deoxygenation of vapors obtained from ablative fast pyrolysis of wheat straw using mesoporous HZSM-5. Fuel Processing Technology, 2019, 194, 106119.	3.7	30
108	Low-Temperature NH3–SCR of NO on Mesoporous Mn0.6Fe0.4/TiO2 Prepared by a Hydrothermal Method. Catalysis Letters, 2014, 144, 395-402.	1.4	29

#	Article	IF	CITATIONS
109	A Rhodium-Based Methane Oxidation Catalyst with High Tolerance to H <sub>2</sub> O and SO <sub>2</sub> . ACS Catalysis, 2020, 10, 1821-1827.	5.5	29
110	Effects of mixing on ammonia oxidation in combustion environments at intermediate temperatures. Proceedings of the Combustion Institute, 2005, 30, 1193-1200.	2.4	28
111	Batch top-spray fluid bed coating: Scale-up insight using dynamic heat- and mass-transfer modelling. Chemical Engineering Science, 2009, 64, 1293-1317.	1.9	28
112	Cell mass and cell cycle dynamics of an asynchronous budding yeast population: Experimental observations, flow cytometry data analysis, and multiâ€scale modeling. Biotechnology and Bioengineering, 2013, 110, 812-826.	1.7	28
113	Superior DeNO x activity of V2O5–WO3/TiO2 catalysts prepared by deposition–precipitation method. Journal of Materials Science, 2014, 49, 2705-2713.	1.7	28
114	Thermal Cracking of Sugars for the Production of Glycolaldehyde and Other Small Oxygenates. ChemSusChem, 2020, 13, 688-692.	3.6	28
115	Spray Drying of Suspensions for Pharma and Bio Products: Drying Kinetics and Morphology. Industrial & Engineering Chemistry Research, 2009, 48, 3657-3664.	1.8	27
116	Structure, activity and kinetics of supported molybdenum oxide and mixed molybdenum–vanadium oxide catalysts prepared by flame spray pyrolysis for propane OHD. Applied Catalysis A: General, 2014, 472, 29-38.	2.2	27
117	Top-spray fluid bed coating: Scale-up in terms of relative droplet size and drying force. Powder Technology, 2008, 184, 318-332.	2.1	26
118	Coupling of Alcohols over Alkaliâ€Promoted Cobalt–Molybdenum Sulfide. ChemCatChem, 2010, 2, 523-526.	1.8	26
119	Modeling char conversion under suspension fired conditions in O2/N2 and O2/CO2 atmospheres. Fuel, 2011, 90, 2224-2239.	3.4	26
120	<i>Operando</i> XAS/XRD and Raman Spectroscopic Study of Structural Changes of the Iron Molybdate Catalyst during Selective Oxidation of Methanol. ChemCatChem, 2019, 11, 4871-4883.	1.8	26
121	Deoxygenation of Wheat Straw Fast Pyrolysis Vapors using HZSM-5, Al <sub>2</sub> O <sub>3</sub> , HZSM-5/Al <sub>2</sub> O <sub>3</sub> Extrudates, and Desilicated HZSM-5/Al <sub>2</sub> O <sub>3</sub> Extrudates. Energy & Fuels, 2019, 33, 6405-6420.	2.5	26
122	Modelling of NOx emissions from pressurized fluidized bed combustion—a parameter study. Chemical Engineering Science, 1997, 52, 1715-1731.	1.9	25
123	Detailed modeling and laser-induced fluorescence imaging of nitric oxide in a NH3-seeded non-premixed methane/air flame. Proceedings of the Combustion Institute, 2002, 29, 2195-2202.	2.4	25
124	Replacement of the foam index test with surface tension measurements. Cement and Concrete Research, 2007, 37, 996-1004.	4.6	25
125	Alkali Resistant Fe-Zeolite Catalysts for SCR of NO with NH3 in Flue Gases. Topics in Catalysis, 2011, 54, 1286-1292.	1.3	25
126	Two-Nozzle Flame Spray Pyrolysis (FSP) Synthesis of CoMo/Al2O3 Hydrotreating Catalysts. Catalysis Letters, 2013, 143, 386-394.	1.4	25

#	Article	IF	CITATIONS
127	NO Reduction over Biomass and Coal Char during Simultaneous Combustion. Energy & Fuels, 2013, 27, 7817-7826.	2.5	25
128	Steam reforming of ethanol over Ni-based catalysts: Effect of feed composition on catalyst stability. International Journal of Hydrogen Energy, 2014, 39, 7735-7746.	3.8	25
129	Poisoning of vanadia based SCR catalysts by potassium: influence of catalyst composition and potassium mobility. Catalysis Science and Technology, 2016, 6, 2249-2260.	2.1	25
130	Noncatalytic Direct Liquefaction of Biorefinery Lignin by Ethanol. Energy & Fuels, 2017, 31, 7223-7233.	2.5	25
131	New insights into the effect of pressure on catalytic hydropyrolysis of biomass. Fuel Processing Technology, 2019, 193, 392-403.	3.7	25
132	Co-processing of wood and wheat straw derived pyrolysis oils with FCC feed—Product distribution and effect of deoxygenation. Fuel, 2020, 260, 116312.	3.4	25
133	Structural dynamics of an iron molybdate catalyst under redox cycling conditions studied with <i>in situ</i> multi edge XAS and XRD. Physical Chemistry Chemical Physics, 2020, 22, 11713-11723.	1.3	25
134	Kinetic NO modelling and experimental results from single wood particle combustion. Fuel, 1997, 76, 671-682.	3.4	24
135	Coupling thermal deactivation with oxidation for predicting the combustion of a solid fuel. Combustion and Flame, 2001, 125, 1341-1360.	2.8	24
136	Post-processing of detailed chemical kinetic mechanisms onto CFD simulations. Computers and Chemical Engineering, 2004, 28, 2351-2361.	2.0	24
137	Small-scale top-spray fluidised bed coating: Granule impact strength, agglomeration tendency and coating layer morphology. Powder Technology, 2007, 176, 156-167.	2.1	24
138	Soot Reactivity in Conventional Combustion and Oxy-fuel Combustion Environments. Energy & Fuels, 2012, 26, 5337-5344.	2.5	24
139	Systematic study on the influence of the morphology of $\hat{I}\pm$ -MoO3 in the selective oxidation of propylene. Journal of Solid State Chemistry, 2015, 228, 42-52.	1.4	24
140	Catalytic Hydropyrolysis of Biomass Using Molybdenum Sulfide Based Catalyst. Effect of Promoters. Energy & Fuels, 2019, 33, 1302-1313.	2.5	24
141	Reactivity of coal char in reducing NO. Combustion and Flame, 2004, 136, 249-253.	2.8	23
142	Process Development of Continuous Glycerolysis in an Immobilized Enzyme-Packed Reactor for Industrial Monoacylglycerol Production. Journal of Agricultural and Food Chemistry, 2007, 55, 7786-7792.	2.4	23
143	Selective Catalytic Reduction of NO <sub>x</sub> with NH <sub>3</sub> on Cu-, Fe-, and Mn-Zeolites Prepared by Impregnation: Comparison of Activity and Hydrothermal Stability. Journal of Chemistry, 2018, 2018, 1-11.	0.9	23
144	The influence of H2O and CO2 on the reactivity of limestone for the oxidation of NH3. Fuel, 2000, 79, 1449-1454.	3.4	22

#	Article	IF	CITATIONS
145	Formation of NO from combustion of volatiles from municipal solid wastes. Combustion and Flame, 2001, 124, 195-212.	2.8	22
146	Effect of the catalyst in fluid bed catalytic hydropyrolysis. Catalysis Today, 2020, 355, 96-109.	2.2	22
147	Catalytic hydropyrolysis of biomass using supported CoMo catalysts – Effect of metal loading and support acidity. Fuel, 2020, 264, 116807.	3.4	22
148	Heat Transfer in a Fixed Bed of Straw Char. Energy & amp; Fuels, 2003, 17, 1251-1258.	2.5	21
149	MnFe/Al2O3 Catalyst Synthesized by Deposition Precipitation for Low-Temperature Selective Catalytic Reduction of NO with NH3. Catalysis Letters, 2015, 145, 1724-1732.	1.4	21
150	Catalytic and gas–solid reactions involving HCN over limestone. AICHE Journal, 1997, 43, 3070-3084.	1.8	20
151	Mixing Effects in the Selective Noncatalytic Reduction of NO. Industrial & Engineering Chemistry Research, 2000, 39, 3221-3232.	1.8	20
152	Activation Energy Distribution of Thermal Annealing of a Bituminous Coal. Energy & Fuels, 2003, 17, 399-404.	2.5	20
153	Dynamic measurement of mercury adsorption and oxidation on activated carbon in simulated cement kiln flue gas. Fuel, 2012, 93, 649-657.	3.4	20
154	Mapping Support Interactions in Copper Catalysts. Topics in Catalysis, 2019, 62, 649-659.	1.3	20
155	Modeling of the molybdenum loss in iron molybdate catalyst pellets for selective oxidation of methanol to formaldehyde. Chemical Engineering Journal, 2019, 361, 1285-1295.	6.6	20
156	Sulfur poisoning and regeneration of Rh-ZSM-5 catalysts for total oxidation of methane. Applied Catalysis B: Environmental, 2020, 277, 119176.	10.8	20
157	Rationalizing an Unexpected Structure Sensitivity in Heterogeneous Catalysis—CO Hydrogenation over Rh as a Case Study. ACS Catalysis, 2021, 11, 5189-5201.	5.5	20
158	Fluidized-Bed Coating with Sodium Sulfate and PVAâ^'TiO <sub>2</sub> , 1. Review and Agglomeration Regime Maps. Industrial & Engineering Chemistry Research, 2009, 48, 1893-1904.	1.8	19
159	Oxy-fuel combustion of millimeter-sized coal char: Particle temperatures and NO formation. Fuel, 2013, 106, 72-78.	3.4	19
160	Site selective adsorption and relocation of SO <sub>x</sub> in deactivation of Cu–CHA catalysts for NH <sub>3</sub> -SCR. Reaction Chemistry and Engineering, 2019, 4, 1081-1089.	1.9	19
161	Performance of mesoporous HZSM-5 and Silicalite-1 coated mesoporous HZSM-5 catalysts for deoxygenation of straw fast pyrolysis vapors. Journal of Analytical and Applied Pyrolysis, 2020, 145, 104712.	2.6	19
162	Characterization of oxide-supported Cu by infrared measurements on adsorbed CO. Surface Science, 2021, 703, 121725.	0.8	19

#	Article	IF	CITATIONS
163	Fluid catalytic co-processing of bio-oils with petroleum intermediates: Comparison of vapour phase low pressure hydrotreating and catalytic cracking as pretreatment. Fuel, 2021, 302, 121198.	3.4	19
164	NH3 oxidation catalyzed by partially sulphated limestone—modelling and experimental work. Fuel, 2004, 83, 237-251.	3.4	18
165	Performance-screening of metal-impregnated industrial HZSM-5/γ-Al2O3 extrudates for deoxygenation and hydrodeoxygenation of fast pyrolysis vapors. Journal of Analytical and Applied Pyrolysis, 2020, 150, 104892.	2.6	18
166	Experimental investigation and modelling of heat capacity, heat of fusion and melting interval of rocks. Thermochimica Acta, 2003, 406, 129-142.	1.2	17
167	Methanolâ€Assisted Autocatalysis in Catalytic Methanol Synthesis. Angewandte Chemie - International Edition, 2020, 59, 18189-18193.	7.2	17
168	A Review of Recent Research on Catalytic Biomass Pyrolysis and Low-Pressure Hydropyrolysis. Energy & Fuels, 2021, 35, 18333-18369.	2.5	17
169	Modeling of temperature profiles in an environmental transmission electron microscope using computational fluid dynamics. Ultramicroscopy, 2015, 152, 1-9.	0.8	16
170	Modeling of in-line low-NOx calciners—a parametric study. Chemical Engineering Science, 2002, 57, 789-803.	1.9	15
171	Evaluation method for the drying performance of enzyme containing formulations. Biochemical Engineering Journal, 2008, 40, 121-129.	1.8	15
172	Alkali resistivity of Cu based selective catalytic reduction catalysts: Potassium chloride aerosol exposure and activity measurements. Catalysis Communications, 2012, 18, 41-46.	1.6	15
173	Trends in the Hydrodeoxygenation Activity and Selectivity of Transition Metal Surfaces. Catalysis Letters, 2014, 144, 1968-1972.	1.4	15
174	Alkali Earth Metal Molybdates as Catalysts for the Selective Oxidation of Methanol to Formaldehyde—Selectivity, Activity, and Stability. Catalysts, 2020, 10, 82.	1.6	15
175	Predicting cold gas-solid flow in a pilot-scale dual-circulating fluidized bed: Validation of computational particle fluid dynamics model. Powder Technology, 2021, 381, 25-43.	2.1	15
176	Pilotâ€scale investigation and <scp>CFD</scp> modeling of particle deposition in lowâ€dust monolithic <scp>SCR DeNOx</scp> catalysts. AICHE Journal, 2013, 59, 1919-1933.	1.8	14
177	Effect of Fe doping on low temperature deNOx activity of high-performance vanadia anatase nanoparticles. Catalysis Communications, 2014, 56, 110-114.	1.6	14
178	A Review and Experimental Revisit of Alternative Catalysts for Selective Oxidation of Methanol to Formaldehyde. Catalysts, 2021, 11, 1329.	1.6	14
179	Validation of the flux number as scaling parameter for top-spray fluidised bed systems. Chemical Engineering Science, 2008, 63, 815-828.	1.9	13
180	Ceria Prepared by Flame Spray Pyrolysis as an Efficient Catalyst for Oxidation of Diesel Soot. Catalysis Letters, 2014, 144, 1661-1666.	1.4	13

#	Article	IF	CITATIONS
181	High Pressure CO Hydrogenation Over Bimetallic Pt–Co Catalysts. Catalysis Letters, 2014, 144, 777-782.	1.4	13
182	Stability of Iron-Molybdate Catalysts for Selective Oxidation of Methanol to Formaldehyde: Influence of Preparation Method. Catalysis Letters, 2020, 150, 1434-1444.	1.4	13
183	Micro-pyrolyzer screening of hydrodeoxygenation catalysts for efficient conversion of straw-derived pyrolysis vapors. Journal of Analytical and Applied Pyrolysis, 2020, 150, 104868.	2.6	13
184	Heterogeneous fixation of N2: Investigation of a novel mechanism for formation of NO. Proceedings of the Combustion Institute, 2009, 32, 1973-1980.	2.4	12
185	Biomass Suspension Combustion: Effect of Two-Stage Combustion on NO <sub><i>x</i></sub> Emissions in a Laboratory-Scale Swirl Burner. Energy & Fuels, 2009, 23, 1398-1405.	2.5	12
186	Selective oxidation of benzyl alcohol in dense CO2: Insight by phase behavior modeling. Journal of Supercritical Fluids, 2012, 63, 199-207.	1.6	12
187	Solvent consumption in non-catalytic alcohol solvolysis of biorefinery lignin. Sustainable Energy and Fuels, 2017, 1, 2006-2015.	2.5	12
188	Hydrodeoxygenation (HDO) of Aliphatic Oxygenates and Phenol over NiMo/MgAl2O4: Reactivity, Inhibition, and Catalyst Reactivation. Catalysts, 2019, 9, 521.	1.6	12
189	Catalytic synthesis of methacrolein <i>via</i> the condensation of formaldehyde and propionaldehyde with <scp>l</scp> -proline. Green Chemistry, 2020, 22, 4222-4230.	4.6	12
190	Influence of experimental protocol on activation energy in char gasification: the effect of thermal annealing. Fuel, 2001, 80, 1029-1032.	3.4	11
191	Investigation of the Anisotropic Behavior of Wood Char Particles during Gasification. Energy & Fuels, 2006, 20, 2233-2238.	2.5	11
192	Deactivation of a CoMo Catalyst during Catalytic Hydropyrolysis of Biomass. Part 1. Product Distribution and Composition. Energy & Fuels, 2019, 33, 12374-12386.	2.5	11
193	Modeling of molybdenum transport and pressure drop increase in fixed bed reactors used for selective oxidation of methanol to formaldehyde using iron molybdate catalysts. Chemical Engineering Science, 2019, 202, 347-356.	1.9	11
194	Liquefaction of Lignosulfonate in Supercritical Ethanol Using Alumina-Supported NiMo Catalyst. Energy & Fuels, 2019, 33, 1196-1209.	2.5	11
195	Insights into the scalability of catalytic upgrading of biomass pyrolysis vapors using micro and bench-scale reactors. Sustainable Energy and Fuels, 2020, 4, 3780-3796.	2.5	11
196	Fluidized-Bed Coating with Sodium Sulfate and PVAâ^'TiO2, 2. Influence of Coating Solution Viscosity, Stickiness, pH, and Droplet Diameter on Agglomeration. Industrial & Engineering Chemistry Research, 2009, 48, 1905-1913.	1.8	10
197	Fluid phase equilibria during propylene carbonate synthesis from propylene oxide in carbon dioxide medium. Journal of Supercritical Fluids, 2013, 82, 106-115.	1.6	10
198	Deactivation of a CoMo Catalyst during Catalytic Hydropyrolysis of Biomass. Part 2. Characterization of the Spent Catalysts and Char. Energy & Fuels, 2019, 33, 12387-12402.	2.5	10

#	Article	IF	CITATIONS
199	Solvent assisted catalytic conversion of beech wood and organosolv lignin over NiMo/γ-Al <sub>2</sub> O <sub>3</sub> . Sustainable Energy and Fuels, 2020, 4, 1844-1854.	2.5	10
200	Kinetic Modeling of Gas Phase Sugar Cracking to Glycolaldehyde and Other Oxygenates. ACS Sustainable Chemistry and Engineering, 2021, 9, 305-311.	3.2	10
201	Impact and attrition shear breakage of enzyme granules and placebo particles-application to particle design and formulation. Powder Technology, 2005, 149, 157-167.	2.1	9
202	Hydrothermally Stable Fe–W–Ti SCR Catalysts Prepared by Deposition–Precipitation. Catalysis Letters, 2014, 144, 1170-1177.	1.4	9
203	Selective Catalytic Reduction of NOx over V2O5-WO3-TiO2 SCR Catalysts—A Study at Elevated Pressure for Maritime Pre-turbine SCR Configuration. Emission Control Science and Technology, 2019, 5, 263-278.	0.8	9
204	Catalytic upgrading of tars generated in a 100ÂkWth low temperature circulating fluidized bed gasifier for production of liquid bio-fuels in a polygeneration scheme. Energy Conversion and Management, 2020, 207, 112538.	4.4	9
205	Investigation of a Mineral Melting Cupola Furnace. Part II. Mathematical Modeling. Industrial & Engineering Chemistry Research, 2003, 42, 6880-6892.	1.8	8
206	The effect of low-NO combustion on residual carbon in fly ash and its adsorption capacity for air entrainment admixtures in concrete. Combustion and Flame, 2010, 157, 208-216.	2.8	8
207	Counteracting Rapid Catalyst Deactivation by Concomitant Temperature Increase during Catalytic Upgrading of Biomass Pyrolysis Vapors Using Solid Acid Catalysts. Catalysts, 2020, 10, 748.	1.6	8
208	Influence of the support on rhodium speciation and catalytic activity of rhodium-based catalysts for total oxidation of methane. Catalysis Science and Technology, 2020, 10, 6035-6044.	2.1	8
209	Catalytic conversion of acetol over HZSM-5 catalysts – influence of Si/Al ratio and introduction of mesoporosity. Catalysis Today, 2021, 365, 301-309.	2.2	8
210	Modeling and Optimization of Multi-functional Ammonia Slip Catalysts for Diesel Exhaust Aftertreatment. Emission Control Science and Technology, 2021, 7, 7-25.	0.8	8
211	Comparative study of reactivity to CO2 of cokes used in stone wool production. Fuel Processing Technology, 2005, 86, 551-563.	3.7	7
212	Precursor Effect on Mn-Fe-Ce/TiO2 Catalysts for Selective Catalytic Reduction of NO with NH3 at Low Temperatures. Catalysts, 2021, 11, 259.	1.6	7
213	Inactivation of a solid-state detergent protease by hydrogen peroxide vapor and humidity. Journal of Biotechnology, 2009, 141, 73-79.	1.9	6
214	Fluidized-Bed Coating with Sodium Sulfate and PVAâ^'TiO2, 3. The Role of Tackiness and the Tack Stokes Number. Industrial & Engineering Chemistry Research, 2009, 48, 1914-1920.	1.8	6
215	Fluid phase equilibria of the reaction mixture during the selective hydrogenation of 2-butenal in dense carbon dioxide. Applied Catalysis A: General, 2012, 443-444, 67-75.	2.2	6
216	Quantification of Formate and Oxygen Coverages on Cu Under Industrial Methanol Synthesis Conditions. Catalysis Letters, 2020, 150, 2447-2456.	1.4	6

#	Article	IF	CITATIONS
217	Promoting Effect of Copper Loading and Mesoporosity on Cu-MOR in the Carbonylation of Dimethyl Ether to Methyl Acetate. Catalysts, 2021, 11, 696.	1.6	6
218	Highly Stable Apatite Supported Molybdenum Oxide Catalysts for Selective Oxidation of Methanol to Formaldehyde: Structure, Activity and Stability. ChemCatChem, 2021, 13, 4954-4975.	1.8	6
219	Investigation of a Mineral Melting Cupola Furnace. Part I. Experimental Work. Industrial & Engineering Chemistry Research, 2003, 42, 6872-6879.	1.8	5
220	A Framework for Modular Modeling of the Diesel Engine Exhaust Gas Cleaning System. Computer Aided Chemical Engineering, 2015, 37, 455-460.	0.3	5
221	Modeling Deactivation of Catalysts for Selective Catalytic Reduction of NO <sub><i>x</i></sub> by KCl Aerosols. Industrial & Engineering Chemistry Research, 2017, 56, 13020-13033.	1.8	5
222	Solvothermal Conversion of Lignosulfonate Assisted by Ni Catalyst: Investigation of the Role of Ethanol and Ethylene Glycol as Solvents. Catalysts, 2018, 8, 502.	1.6	5
223	Mathematical Modelling and Simulation of a Trickle-Bed Reactor for Hydrotreating of Petroleum Feedstock. International Journal of Chemical Reactor Engineering, 2019, 17, .	0.6	5
224	Comprehensive development, uncertainty and sensitivity analysis of a model for the hydrolysis of rapeseed oil. Computers and Chemical Engineering, 2020, 133, 106631.	2.0	5
225	Ethanol-selective catalytic reduction of NO by Ag/Al2O3 catalysts: Activity and deactivation by alkali salts. Applied Catalysis B: Environmental, 2012, 127, 323-329.	10.8	4
226	The Influence of Active Phase Loading on the Hydrodeoxygenation (HDO) of Ethylene Glycol over Promoted MoS2/MgAl2O4 Catalysts. Topics in Catalysis, 2019, 62, 752-763.	1.3	4
227	Hydroxyapatite supported molybdenum oxide catalyst for selective oxidation of methanol to formaldehyde: studies of industrial sized catalyst pellets. Catalysis Science and Technology, 2021, 11, 970-983.	2.1	4
228	Co-firing of Coal with Biomass and Waste in Full-Scale Suspension-Fired Boilers. , 2013, , 781-800.		4
229	Modelling of an adiabatic trickle-bed reactor with phase change. Computer Aided Chemical Engineering, 2017, 40, 115-120.	0.3	3
230	Methanolâ€Assisted Autocatalysis in Catalytic Methanol Synthesis. Angewandte Chemie, 2020, 132, 18346-18350.	1.6	3
231	Modelling of In-Line Low-NOX Calciners—NOX Emission. Chemical Engineering Research and Design, 2003, 81, 537-548.	2.7	2
232	Comments to "Analysis of constant rate period of spray drying of slurry―by Liang et al., 2001. Chemical Engineering Science, 2006, 61, 2096-2100.	1.9	2
233	Post-treatment of Fly Ash by Ozone in a Fixed Bed Reactor. Energy & amp; Fuels, 2009, 23, 280-285.	2.5	2
234	SO2 Oxidation Across Marine V2O5-WO3-TiO2 SCR Catalysts: a Study at Elevated Pressure for Preturbine SCR Configuration. Emission Control Science and Technology, 2018, 4, 289-299.	0.8	2

#	Article	IF	CITATIONS
235	A simplified kinetic and mass transfer modelling of the thermal hydrolysis of vegetable oils. Computer Aided Chemical Engineering, 2017, 40, 1177-1182.	0.3	1
236	Multi-scale modeling for prediction of distributed cellular properties in response to substrate spatial gradients in a continuously run microreactor. Computer Aided Chemical Engineering, 2012, , 545-549.	0.3	1
237	Application of a Mathematical Model of a Mineral Melting Cupola. Industrial & Engineering Chemistry Research, 2003, 42, 6893-6897.	1.8	0
238	Electron Microscopy Study of the Deactivation of Nickel Based Catalysts for Bio Oil Hydrodeoxygenation. Microscopy and Microanalysis, 2014, 20, 458-459.	0.2	0
239	Pressure Induced Effects During In Situ Characterization of Supported Metal Catalysts. Microscopy and Microanalysis, 2018, 24, 240-241.	0.2	0